COMPRESSION OF INTERSTELLAR CLOUDS IN SPIRAL DENSITY-WAVE SHOCKS

Paul R. Woodward
Leiden Observatory, The Netherlands, and
Lawrence Livermore Laboratory, Livermore, Calif.

ABSTRACT

A mechanism of triggering star formation by galactic shocks is discussed.

The possibility that shocks may form along spiral arms in the gaseous component of a galactic disk is by now a familiar feature of spiral wave theory. It was suggested by Roberts (1969) that these shocks could trigger star formation in narrow bands forming a coherent spiral pattern over most of the disk of a galaxy. In this paper I will report some results of computer simulations of such a triggering process for star formation.

I begin the simulations with a spherical "standard" interstellar cloud in an interarm region. The cloud has a mass of 524 $M_\odot$, radius of 15 pc, and density of 1.5 m_H cm^{-3}. Reasons for this choice of the initial cloud are discussed in an earlier article (Woodward 1976). The results for this cloud can be scaled to different cloud masses by multiplying all lengths and times by a common factor. The cloud was followed numerically using the BBC code (cf Sutcliffe 1973, Noh and Woodward 1976) as it passed through a spiral arm shock in the surrounding isothermal gas. This intercloud gas, with a sound speed of 8.6 km/sec, increases in density from about 0.02 to 0.11 m_H cm^{-3} across the spiral arm shock.

In figure 1 the cloud is shown near the beginning of the computation as it is entering the spiral arm. The cloud is viewed and velocities are displayed in a frame of reference in which the interarm gas moves to the right at 1.5 km/sec. In this frame the intercloud gas of the spiral arm rushes into the cloud at about 15.5 km/sec. In figure 1 the spiral arm shock is delineated by the closely spaced density contours at the bottom left. A bow shock ahead of the cloud has formed because the cloud moves supersonically with respect to the intercloud gas of the spiral arm. The ram pressure from this motion causes the shock driven into the cloud to be strongest at the front. The resulting flattening of the cloud is already apparent in figure 1, about 3×10^6 years after the cloud entered

W. B. Burton (ed.), The Large-Scale Characteristics of the Galaxy, 159–164.

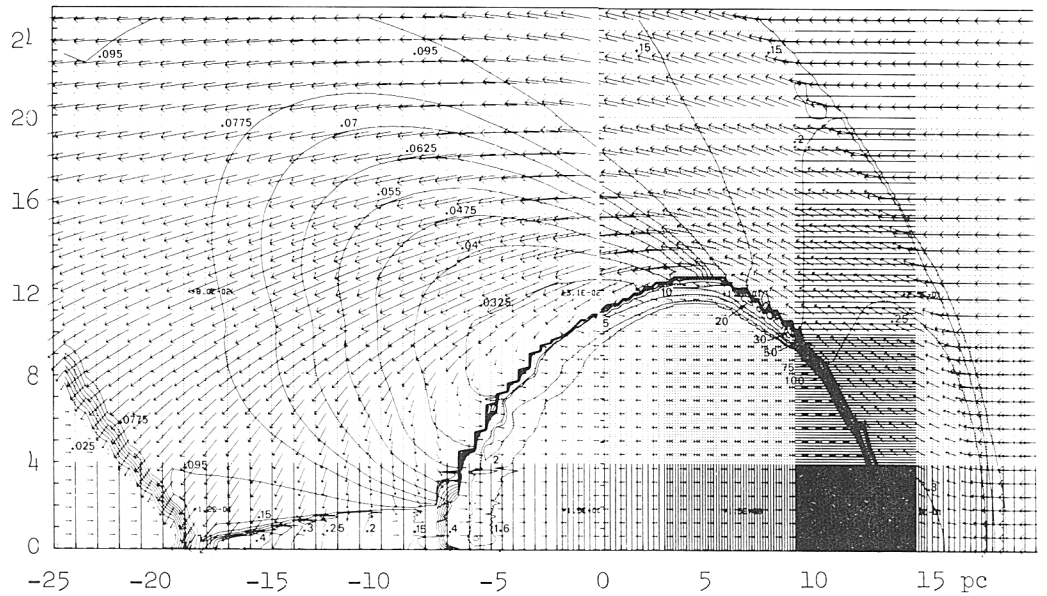

Figure 1. An interstellar cloud shown 3×10^6 yrs after encountering a spiral arm shock. See text for details of display format.

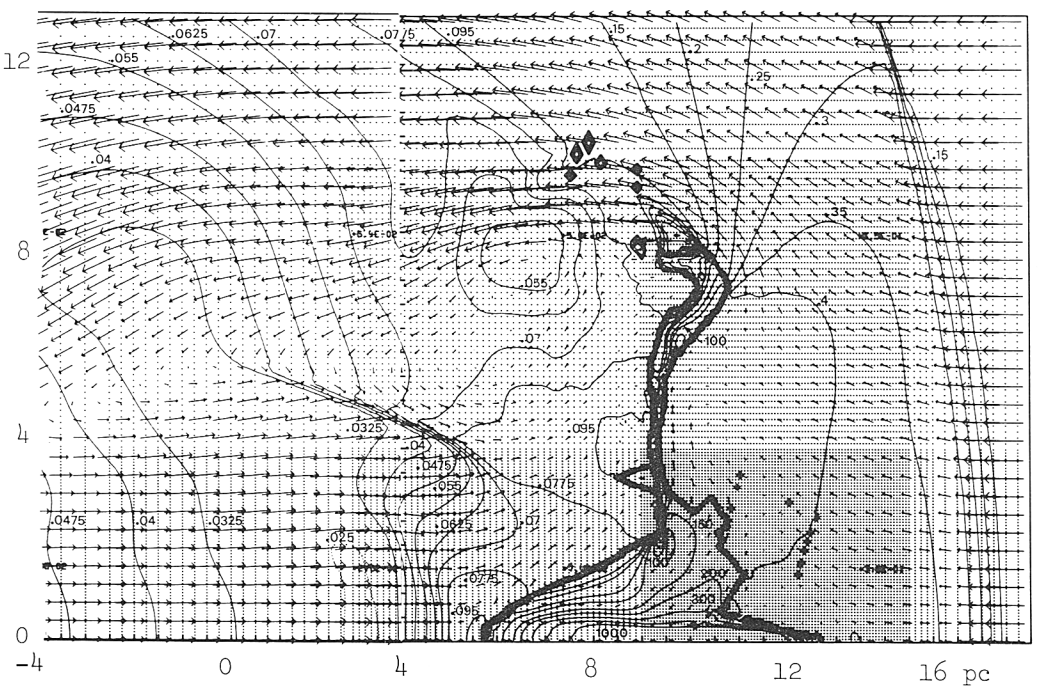

Figure 2. The interstellar cloud of figure 1 shown 7×10^6 yrs after encountering the spiral arm shock.

https://doi.org/10.1017/S0074180900014406 Published online by Cambridge University Press

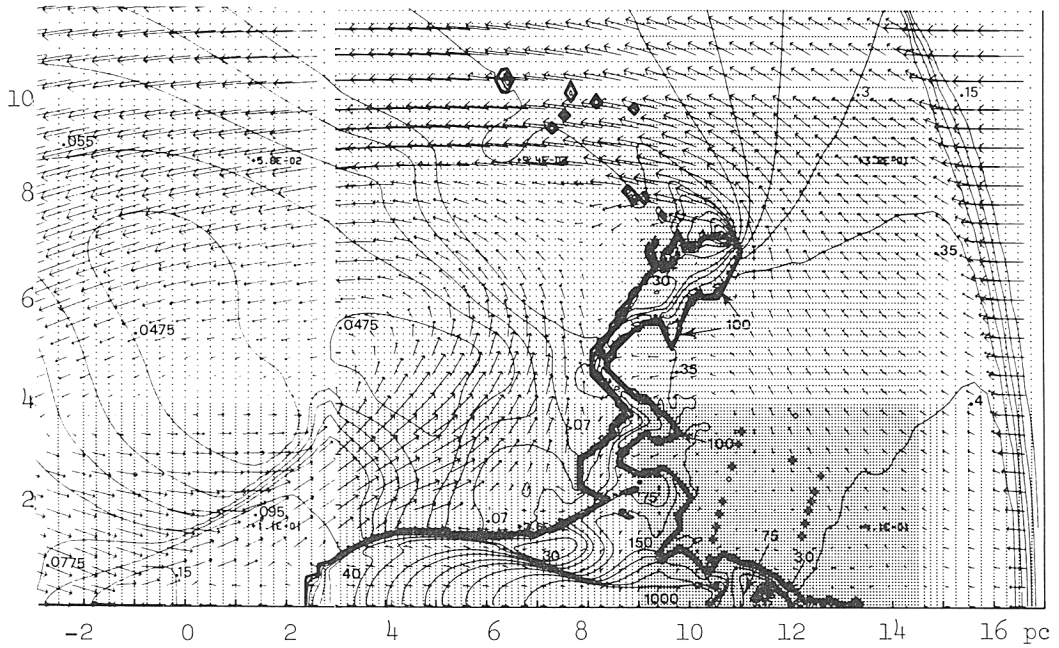

Figure 3. The interstellar cloud of figure 1 shown 8×10^6 yrs after encountering the spiral arm shock.

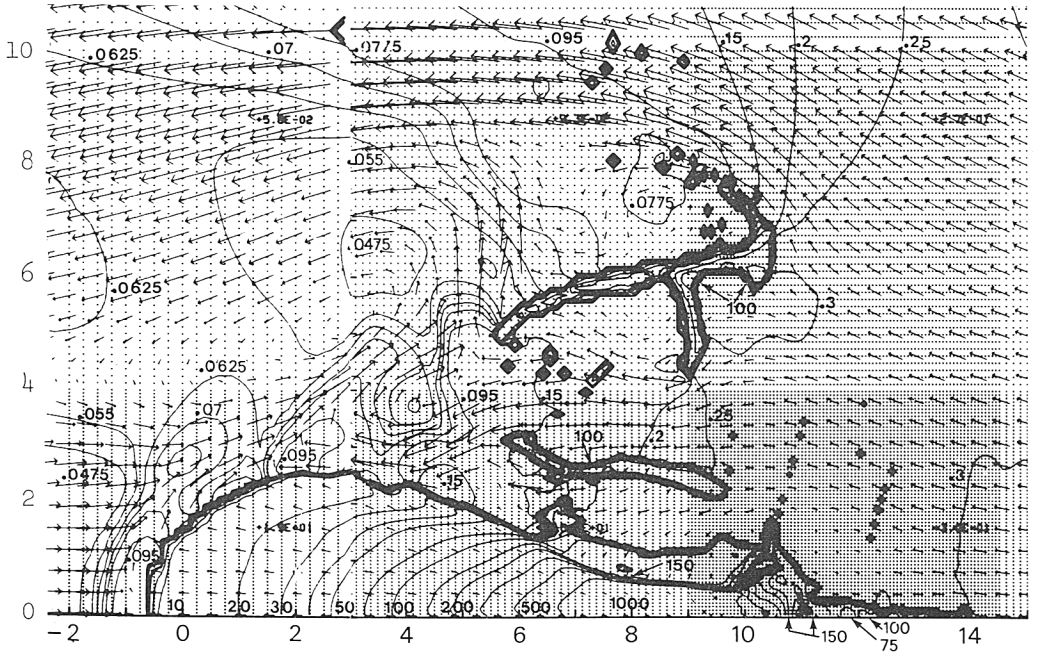

Figure 4. The interstellar cloud of figure 1 shown 9×10^6 yrs after encountering the spiral arm shock.

https://doi.org/10.1017/S0074180900014406 Published online by Cambridge University Press

the spiral arm. The density contours tracing the cloud boundary in the figure give it a step-like appearance. This is due to the plotting routine; the actual data is smooth. The computational grid extends beyond the figure and contains about 34,000 zones. Zones are indicated by dots, which are so close together near the front of the cloud that the region appears completely black in figure 1.

The Kelvin-Helmholtz, or "water-wave," instability which was seen in earlier computations (Woodward 1976) is not seen in figure 1. The isothermal equation of state used here for the intercloud gas results in a supersonic flow of this gas around the cloud. This, together with the effective numerical viscosity of the boundary treatment, causes the Kelvin-Helmholtz instability to be suppressed (cf Gerwin 1968). The Rayleight-Taylor instability of the front cloud surface is apparent from the distortions of that surface in figure 2, which shows the cloud 7×10^6 years after it entered the spiral arm. Here the cloud has been entirely flattened. Focussed flow of shocked cloud gas toward the symmetry axis has given rise to a maximum density there, about 10^4 m_H cm^{-3}. Now that propagation of the shock through the cloud has communicated the high pressure associated with this dense gas on the symmetry axis to the back of the cloud, an expansion into the low-pressure intercloud region behind the cloud has begun. This causes a dense, expanding tail to form along the symmetry axis behind the densest part of the cloud. This tail is more clearly visible in figure 3, where the cloud is shown 8×10^6 years after entering the spiral arm. As the flattened sheet of cloud gas shown in figure 2 expands into the low pressure region behind it, its great acceleration causes rapid growth of the Rayleigh-Taylor instability. This gives rise to the distortion of the sheet in figure 3 and its eventual break up in figure 4, 9×10^6 years after entry into the spiral arm.

The cloud in figure 4 has several features characteristic of this sort of shock-driven implosion. It is elongated in the direction of motion relative to the surrounding intercloud gas. At the front end the density is highest, and this is the preferred location for star formation in the cloud. This model therefore leads to a picture where stars form preferentially at the edges of dense clouds, rather than at their centers. The model therefore ties in naturally with shock-driven star formation mechanisms which demand the presence of a first generation of massive stars in order to initiate a chain reaction of star formation. Thus young stars formed at the head of the cloud in figure 4 could compress the cloud further by means of strong stellar winds, expanding H II regions or supernova explosions. These mechanisms, which all involve a shock compression from one side of the cloud, could drive a wave of star formation down the length of the cloud.

The ionization-driven mechanism is illustrated by the dense clouds near the H II region W3. These are shown in figure 5. The integrated CO brightness temperature is shown within the dashed box, sampled at single-beam intervals. These observations were made with the Columbia 4-ft telescope, with a resolution of 8', by Cong and Thaddeus (1977, private communication). Longitude values are shown along the galactic

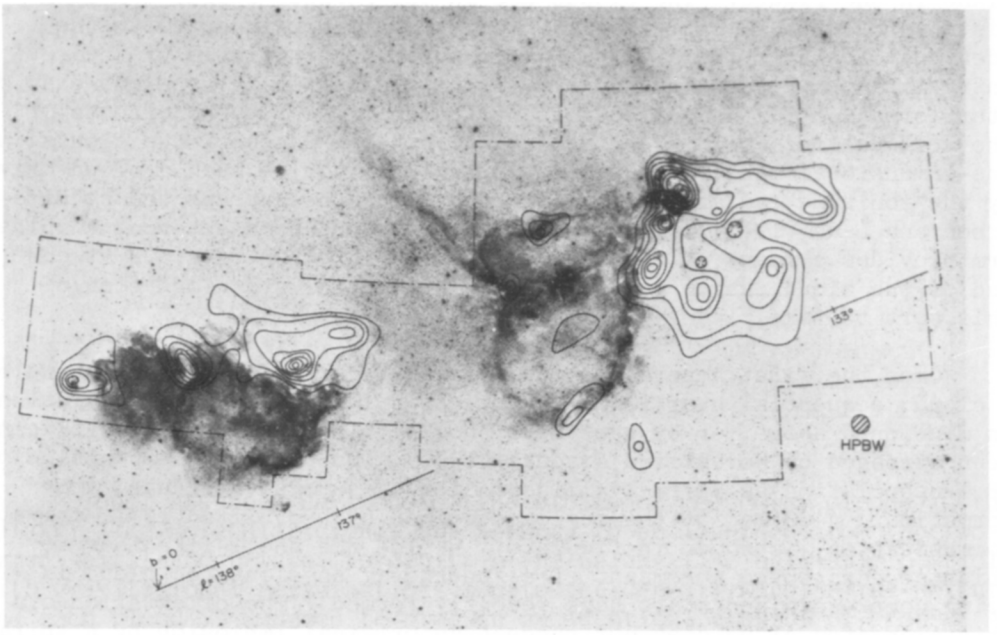

Figure 5. Dense clouds near the H II region W3. Contours of CO brightness temperature from observations of Cong and Thaddeus.

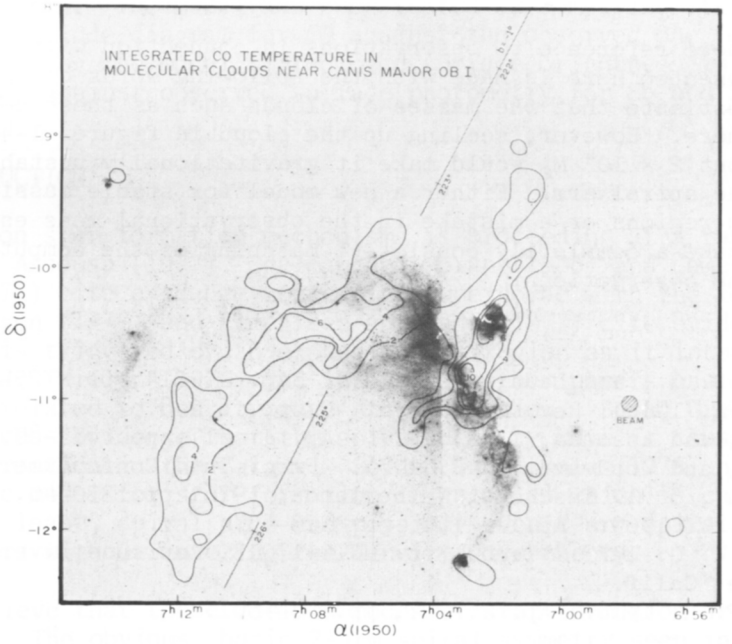

Figure 6. CO map of the Canis Major OB I region (distance 1.15 kpc) from observations of Leo Blitz.

https://doi.org/10.1017/S0074180900014406 Published online by Cambridge University Press

plane in the figure. The clouds are in the Perseus spiral arm at a distance of about 2 kpc. Their orientation is consistent with the idea that the star formation at their edges was initiated by their entry into the Perseus spiral arm. In any case, it is apparent that star formation in these clouds is now being driven by the effects of the H II regions which are pressing against the edges of the clouds. A one-dimensional model of a wave of star formation in such a cloud driven by the ionizing radiation of massive stars has been presented by Elmegreen and Lada (1977). The implosion of a cloud upon entering a spiral arm provides a means of obtaining a first generation of stars at one end of the cloud, which may then cause sequential star formation of this sort to take place.

Once the first generation of massive stars is formed at one end of a cloud, sequential star formation may be driven by ionizing radiation, as mentioned above, or by supernova shocks. This latter alternative has been stressed by Herbst and Assousa (1977), who present the Canis Major OB I association as a likely illustration of supernova-induced star formation. A CO map of the region obtained by Leo Blitz (1977, private communication) is shown in figure 6. Beside the shell-like feature which appears to be a remnant of a supernova, an elongated cloud is being compressed and stars have recently formed. The orientation of this elongated cloud does not suggest an original implosion by a spiral arm shock. Nevertheless, it illustrates how a star formation chain reaction might be triggered and maintained in a cloud which is imploded upon entering a spiral arm.

The above reference to observations in connection with the calculations presented here is made with the following words of caution. CO observers estimate that the masses of clouds such as those near W3 are 10^5 $M_\odot$ or more. However, scaling up the cloud in figures 1-4 beyond a mass of about 2×10^4 $M_\odot$ would make it gravitationally unstable before entering the spiral arm. Either a new model for stable massive clouds in interarm regions or a mistake in the observational mass estimate is needed to make a completely consistent matching of the computer simulations to the observations.

REFERENCES

Elmegreen, B. G., and Lada, C. J. 1977. Ap. J. 214, pp. 725-41.
Gerwin, R. A. 1968. Rev. Mod. Phys. 40, pp. 652-8.
Herbst, W., and Assousa, G. E. 1977. Ap. J. 217, pp. 473-87.
Noh, W. F., and Woodward, P. R. 1976. Proc. Int. Conf. Numer. Methods Fluid Dyn., 5th, Enschede, Netherlands, 1976, pp. 330-40.
Roberts, W. W. 1969. Ap. J. 158, pp. 123-43.
Sutcliffe, W. G. 1973. Tech. Rpt. UCID-17013, Lawrence Livermore Lab, Livermore, Calif.
Woodward, P. R. 1976. Ap. J. 207, pp. 484-501.